J. Fluid Mech. (1968), *vol.* 34, *part* 2, *pp.* 241–261
Printed in Great Britain

Linearized analysis of constant-property duct flows

By F. A. WILLIAMS

Department of the Aerospace and Mechanical Engineering Sciences,
University of California, San Diego, La Jolla, California

(Received 24 August 1967 and in revised form 7 May 1968)

The conservation equations describing steady, incompressible flow in a variable-area duct with mass transfer occurring at its walls are simplified by linearizing the inertial and convective terms. Solutions to a large class of problems can be obtained by means of the general method which is presented. Particular examples considered are entrance flow with heat transfer to an isothermal wall in the presence of mass addition, constant rate of injection of a foreign gas through the wall, vaporization and sublimation of a volatile wall material, and gas-phase combustion of a fuel which enters the duct from its wall. Comparison of the present results with previous work and with new experimental results is discussed for the first of these applications. It is concluded that the present results for velocity and pressure fields are likely to be accurate for small values of the Reynolds number based on wall injection velocity, that the present results for temperature and composition fields are likely to be accurate in the absence of wall mass transfer, and that in the absence of wall mass transfer the linearization technique is likely to exhibit its highest accuracy for flows with uniform entrance conditions.

1. Introduction

Non-linearity is the major obstacle in deriving solutions to the Navier–Stokes equations. Numerous techniques have been suggested for producing linear approximations to these equations. This paper concerns a particular linear approximation that resembles the simple approximation of Oseen (1910), which was modified and extended by Lewis & Carrier (1949), Carrier (1962) and by others. Originally developed for external flows, approximations of this type have occasionally been applied to internal flows. By means of one such approximation, Sparrow, Lin & Lundgren (1964) recently achieved remarkable success in describing the manner in which velocity and pressure fields develop from a uniform inlet velocity distribution to a Poiseuille distribution, in constant-area, impermeable-wall ducts of circular and infinite-strip cross-sections. This success prompted the study reported herein, the objectives of which were first to investigate the extent to which this type of linearization can be generalized for application to other types of constant-property duct flows and second to estimate the accuracy of the resulting generalizations in various cases.

Since the Oseen approximation for external flows commonly is restricted to low Reynolds numbers, it may be worth emphasizing at the outset that the

Reynolds number will not be assumed to be low, and the boundary-layer equations will be assumed to describe properly the duct flows considered herein. Heuristic justifications have been given (e.g. Williams 1963) for using the boundary-layer equations at moderate or high Reynolds numbers in impermeable-wall duct flows, provided only that the length-to-width ratio of the duct is sufficiently large. There seems to be no reason for smoothly varying rates of wall injection to nullify the arguments, provided that the injection velocity is small in comparison with the cross-sectional average of the axial velocity. Most of the viscous duct-flow analyses that have appeared in the literature employ the boundary-layer equations. However, we should hasten to point out that there may well exist flow regions in which these equations are not valid. For example, boundary-layer analyses of flow development from a uniform inlet velocity profile yield an infinite axial pressure gradient at the inlet plane, a clear indication that the approximation breaks down at the entrance. The difficulties that arise (e.g. modifications in proper boundary conditions) when the full Navier–Stokes equations are used for resolving these troubles have been discussed by a number of authors (e.g. Cole 1968); accordingly, we restrict our attention almost entirely to cases in which the boundary-layer approximation is acceptable. Our criteria for success of a theory therefore are agreement with exact solutions to the boundary-layer equations and also agreement with experimental results that are not affected by flow regions in which the boundary-layer equations are inapplicable. However, we shall also discuss briefly in §3 new experimental evidence pointing toward possible failure of the boundary-layer equations in certain duct flows.

Duct flows are more difficult to analyze than external flows in that the streamwise pressure gradient is not known in advance when the solution to the boundary-layer equations is sought. Additional approximations therefore often are needed to render analysis of duct flows tractable. The core of the linear approximation considered herein, whose development as referenced by Sparrow *et al.* (1964) appears to have occurred largely in Soviet literature, involves the replacement

$$u_i \partial/\partial x_i \rightarrow U(x)\,\partial/\partial x + E(x)$$

in the inertial and convective terms. Here x is the streamwise co-ordinate. Variations on the theory arise by using different integral conditions for determining the functions $U(x)$ and $E(x)$. Choosing $U(x)$ and $E(x)$ in such a way that an integral of the momentum conservation equation and an integral of the mechanical energy conservation equation are both satisfied was found by Sparrow *et al.* (1964) to lead to excellent agreement with velocity and pressure fields measured experimentally (for flow development in tubes of circular cross-section) and calculated numerically by finite-difference solutions to the boundary-layer equations (for flow development in two-dimensional channels). If the numerical, finite-difference solutions given by Hornbeck (1963) for the boundary-layer equations describing flow development in a circular tube are compared with this linearized solution, then one again finds excellent detailed agreement. These results, which are surprising at high Reynolds numbers, will be inferred from the following analyses to be peculiar to flow development in ducts *with*

uniform initial velocity profiles. Although the accuracy of the results of the linear analysis appears in general to become progressively poor with increasing deviation of conditions from those of the relatively simple problems analyzed previously, there is a range of conditions over which the theory is reasonably accurate. For uniform entrance profiles, reasonable accuracy is achieved for the velocity field when the injection Reynolds number is small, and for temperature and composition fields when there is no wall mass transfer.

The general theory is outlined in the following section. Four different types of applications are considered in the appendices, without regard for the accuracy of the theory in each class of applications. Except for the first class of applications, there appear to be no published results with which the present theory can be compared to ascertain its accuracy. The greatly extended range of applicability (although perhaps with poor accuracy) thus implied, may in itself contribute to the value of the theory. Comparison with previous work is possible for a number of applications in the first class. Such comparisons are given in the third section and are used to draw conclusions concerning the accuracy of the theory.

2. Theory

The equations with which we begin are the continuity equation and the boundary-layer forms of the momentum equation (with inertial, pressure-gradient and viscous terms) and of a set of diffusion equations (with convective and diffusive terms). The diffusion equations for the dependent variables β_i describe the temperature field, composition fields or in a chemically reacting system fields defined by linear, temperature-composition combinations that effect the elimination of chemical source terms in the manner demonstrated by Williams (1965, pp. 9–13). We reserve vector notation ($\mathbf{r}$, $\boldsymbol{\nabla}$, etc.) for the two-dimensional space orthogonal to the flow (x) direction. The wall of the variable-area duct is given by a curve $C(x)$ in the plane orthogonal to x. We assume that the cross-sections of the duct are geometrically similar in the sense that two Cartesian co-ordinates orthogonal to x can be multiplied by a function of x to produce a stretched transverse co-ordinate system in which the wall curve is $C_0 = C(0)$ for all x. Curvature of the centre line and twist of the geometrically similar cross-sections are excluded. The unit of length is taken to be the square root of the duct cross-sectional area at $x = 0$, the unit of mass is chosen so that the density is unity, and the unit of time is then chosen so that the coefficient of viscosity is unity. All quantities appearing in this paper are therefore non-dimensional (except for certain of the quantities β discussed in the appendices). The conservation equations (in stretched transverse co-ordinates) then become

$$b^2 u_x - bb'\mathbf{r}.\boldsymbol{\nabla}u + b\boldsymbol{\nabla}.\mathbf{v} = 0, \tag{1a}$$

$$b^2 u u_x - bb'u\mathbf{r}.\boldsymbol{\nabla}u + b\mathbf{v}.\boldsymbol{\nabla}u = -b^2 p' + \nabla^2 u, \tag{1b}$$

$$b^2 u \beta_{ix} - bb'u\mathbf{r}.\boldsymbol{\nabla}\beta_i + b\mathbf{v}.\boldsymbol{\nabla}\beta_i = \alpha\nabla^2\beta_i, \tag{1c}$$

where a subscript x denotes a partial derivative with respect to x, a prime denotes a total derivative with respect to x, the quantity $b(x)$ denotes the square root of

the cross-sectional area of the duct and $\alpha = \rho D = \lambda/c_p$ denotes the diffusivity for heat and mass, which is assumed to be the same for all β fields but need not equal the diffusivity for momentum.

The unknown pressure gradient can be eliminated from the momentum equation by performing an integration over the cross-sectional area and by using the no-slip condition at the wall. Unless both $b' \neq 0$ and $\mathbf{v}.\mathbf{n} \neq 0$ at the wall, the correct no-slip condition is $u = 0$. When both $b' \neq 0$ and $\mathbf{v}.\mathbf{n} \neq 0$ at the wall, the error involved in using $u = 0$ as the wall boundary condition is of an order of magnitude that is no greater than b'^2 in all of the formulas except for (2), in which a term involving $b'(\mathbf{v}.\mathbf{n})^2$ should occur. We assume in the development that b' is sufficiently small for terms of order b'^2 to be negligible, and we therefore use $u = 0$ as the no-slip condition. In this manner, the relationship

$$b^2 p' = \oint \mathbf{n}.\nabla u \, ds - \left(b^2 \iint u^2 dA \right)_x \tag{2}$$

is obtained, where $\oint$ denotes a closed-line integral around the wall curve C_0 whose outward pointing normal is denoted by $\mathbf{n}$, and $\iint$ denotes a surface integral over the total cross-sectional area of the duct. The substitution of (2) into (1b) yields an integrodifferential equation which does not involve p'.

The linearization discussed in the introduction is achieved by replacing the left-hand sides of (1b) and (1c) by

$$U(u, \beta_i)_x + (E, E_i),$$

where U, E and E_i are independent of the transverse co-ordinates. We shall take $E_i = 0$, since it can be shown that the solutions for the β_i fields are independent of the choice of $E_i(x)$. However, $E(x)$ will be retained in the momentum equation, because otherwise erroneous pressure gradients would be obtained.

The integral of (1a) over the cross section shows that the linearized form of (2) becomes

$$E + b^2 p' = \oint \mathbf{n}.\nabla u \, ds + (U/b) \oint \mathbf{n}.\mathbf{v} \, ds + (2Ub'/b) \iint u \, dA. \tag{2'}$$

The approximation

$$b^2 \iint u \, dA = U \tag{3}$$

is introduced (only) into the last term in (2'), yielding a manageable formula for p', and reducing (1b) and (1c) to

$$U u_x = -2U^2 b'/b^3 - \oint \mathbf{n}.\mathbf{v} \, ds \, U/b - \oint \mathbf{n}.\nabla u \, ds + \nabla^2 u \tag{4}$$

and

$$U \beta_{ix} = \alpha \nabla^2 \beta_i. \tag{5}$$

The equations are linear in the absence of the approximation given in (3), but a troublesome variable coefficient appears (unless b'/b is constant) if (3) is not introduced. In (4), the first two terms on the right-hand side account for the change of momentum due to area convergence and mass addition at the walls, respectively; the approximation in (3) affects only the first of these two terms.

In terms of the variable

$$\xi \equiv \int_0^x U^{-1} dx, \tag{6}$$

we define the function

$$F(\xi) = -2U^2 b'/bu_0 - \oint \mathbf{n}.\mathbf{v} ds\, U/bu_0, \tag{7}$$

where u_0 is the value of u at $x = 0$, which we assume to be independent of the transverse co-ordinates. The solution to (4) then can be written in the form

$$u = u_0 \sum_{j=0}^{\infty} c_j g_j \exp(-\alpha_j^2 \xi) \left[1 + \int_0^{\xi} F(\xi) \exp(\alpha_j^2 \xi) d\xi\right], \tag{8}$$

where g_j are eigenfunctions and α_j are eigenvalues for the integrodifferential equation

$$\alpha_j^2 g_j - \oint \mathbf{n}.\nabla g_j ds + \nabla^2 g_j = 0, \quad (j = 0, 1, 2, \ldots) \tag{9}$$

subject to the boundary condition

$$g_j = 0 \quad \text{on} \quad C_0, \quad (j = 0, 1, 2, \ldots),$$

and the coefficients c_j are given by

$$\left.\begin{aligned} c_0 &= 1 \Big/ \iint g_0 dA, \\ c_j &= -c_0 \iint g_j g_0 dA \Big/ \iint g_j^2 dA, \quad (j = 1, 2, \ldots). \end{aligned}\right\} \tag{10}$$

The function g_0 is proportional to the fully developed velocity profile ($\alpha_0 = 0$), while g_j for $j = 1, 2, \ldots$, are mutually orthogonal and also orthogonal to unity. Equation (9) has been solved by Sparrow *et al.* (1964) for the circular tube and for the two-dimensional channel, and the corresponding eigenfunctions and eigenvalues are listed by them. All of the eigenvalues except α_0 are positive.

Equation (8) already provides solutions to a variety of problems. In the simplest variation of the theory U can be set constant, equal to its value at $x = 0$. Then $F(\xi)$ is a known function, provided that the duct area and the wall injection rate are specified functions of x. In view of the fact that g_j, α_j and hence c_j have already been determined for circular and strip cross sections, it follows that the velocity distribution can be calculated directly from (8) for arbitrarily specified duct area variation and wall injection rate, in these geometries. Refinements to this calculation can be made by allowing U to vary with x. One may set

$$U = u_0 - \int_0^x b \oint \mathbf{n}.\mathbf{v} ds dx \tag{11}$$

to satisfy an over-all continuity equation with the approximate convective velocity. Alternatively, one may allow U to vary with x in such a way that a linearized over-all mechanical energy conservation equation is satisfied in addition to the linearized over-all momentum equation, thereby obtaining results

which for the straight duct without mass addition are equivalent to those of Sparrow *et al.* (1964). Another alternative is to allow U to satisfy (11) but introduce an x-dependent viscosity coefficient that varies with x in such a way that the linearized over-all mechanical energy and momentum equations are both satisfied; the straight-duct, no-mass-addition limit of this result will also be identical to the previously successful result. These last two refinements will not be carried out here.

There are systems in which the wall injection rate is influenced by temperature and composition fields within the duct, so that $F(\xi)$ in (8) is not known until the solution to (5) is obtained. The solution to (5) will depend on the boundary conditions that are to be applied at $x = 0$ and at the duct wall. We assume that at $x = 0$, $\beta_i = \beta_{i0}$, a known constant, and that the wall boundary condition can be expressed in the form

$$\sum_i [A_{ki}\beta_{iw} + B_{ki}(\mathbf{n}.\nabla\beta_i)_w] = C_k, \tag{12}$$

where all of the quantities A_{ki}, B_{ki} and C_k are permitted to be functions of x, and the subscript w identifies conditions at the wall. If $F(\xi)$ is known then there are the same total number of k's as i's. If $F(\xi)$ is not known, the total number of k's exceeds the total number of i's by one; the additional equation determines the injection rate which appears in C_k and/or A_{ki}. In the following discussion, we assume that an unknown injection rate can be made to appear in just one equation, whence there exists an independent set of equations with known coefficients. It can be seen from (12) that coupling among the various β_i fields is permitted through the boundary conditions. A wide class of problems obeys the restrictions imposed here; specific examples can be found in the appendices.

Following a suggestion of P. A. Libby, we shall assume that the solutions $G_A(z, \mathbf{r})$ and $G_B(z, \mathbf{r})$ to the following two basic problems are known:

$$(G_{A,B})_z = \nabla^2 G_{A,B}, G_{A,B} = 0 \quad \text{for} \quad z \leqslant 0, \quad \left\{\begin{matrix} G_{Aw} = 1 \\ (\mathbf{n}.\nabla G_B)_w = 1 \end{matrix}\right\} \quad \text{for} \quad z > 0. \tag{13}$$

Solutions for the wall conditions given in (13) are often available when solutions for other wall conditions are not. Solutions may be written in terms of expansions analogous to but simpler than that defined in (8), (9) and (10). The solution to (5), subject to the condition $\beta_i = \beta_{i0}$ at $x = 0$, can then be written in terms of either G_A or G_B as

$$\beta_i = \beta_{i0} + \int_0^{\alpha\xi} G_A(\alpha\xi - z, \mathbf{r})\beta_{iwz}\,dz \tag{14a}$$

or

$$\beta_i = \beta_{i0} + \int_0^{\alpha\xi} G_B(\alpha\xi - z, \mathbf{r})(\mathbf{n}.\nabla\beta_i)_{wz}\,dz, \tag{14b}$$

in which the subscript wz implies that the wall value is to be differentiated with respect to $\alpha\xi$, and then ξ is to be set equal to z/α in the function obtained from the differentiation.

For each β_i, we adopt the representation given by either (14a) or (14b). The choice is based on the form of the boundary condition (12). If for some i, $B_{ki} = 0$ for all k and x, then we use (14a) for this i; if for another i, $A_{ki} = 0$ for all k and x,

then we adopt (14*b*) in this case. If for a given i, both A_{ki} and B_{ki} differ from zero somewhere, then the choice is open, but generally (14*a*) is to be favoured when $|A_{ki}| > |B_{ki}|$ for most k and x, and vice versa. The coupling functions β_i are thus divided into two classes, (A) and (B), according to whether (14*a*) or (14*b*) is employed, respectively.

The boundary condition (12) remains to be satisfied. In view of (14), this condition can be written as

$$\sum_{i\in(A)}\left\{A_{ki}(\beta_{iw}-\beta_{i0})+A_{ki}\beta_{i0}+B_{ki}\int_0^{\alpha\xi}[\mathbf{n}.\nabla G_A(\alpha\xi-z,\mathbf{r})]_w(\beta_{iw}-\beta_{i0})_z dz\right\}$$
$$+\sum_{i\in(B)}\left\{A_{ki}\beta_{i0}+A_{ki}\int_0^{\alpha\xi}[G_B(\alpha\xi-z,\mathbf{r})]_w(\mathbf{n}.\nabla\beta_i)_{wz}dz+B_{ki}(\mathbf{n}.\nabla\beta_i)_w\right\}=C_k. \quad (15)$$

The unknowns in (15) are $\beta_{iw}-\beta_{i0}$ and $(\mathbf{n}.\nabla\beta_i)_w$, which can be considered to be components of a vector function $\boldsymbol{\beta}$ of $\alpha\xi$. Equation (15) then can be written in matrix notation as

$$\mathscr{A}(\alpha\xi)\,\boldsymbol{\beta}(\alpha\xi)+\int_0^{\alpha\xi}\mathscr{B}(\alpha\xi,z)\,(d/dz)\,\boldsymbol{\beta}(z)\,dz=\mathbf{C}(\alpha\xi), \quad (15')$$

where the definitions of the square matrices $\mathscr{A}$ and $\mathscr{B}$ and of the vector $\mathbf{C}$ are apparent by comparison. Equation (15′) is obviously a matrix integral equation for $\boldsymbol{\beta}(\alpha\xi)$. Its solution may be calculated from the iterative formula

$$\boldsymbol{\beta}^{(n)}(\alpha\xi)=\mathscr{A}^{-1}(\alpha\xi)\,\mathbf{C}(\alpha\xi)-\int_0^{\alpha\xi}\mathscr{A}^{-1}(\alpha\xi)\,\mathscr{B}(\alpha\xi,z)\,(d/dz)\,\boldsymbol{\beta}^{(n-1)}(z)\,dz, \quad (16)$$

with $\boldsymbol{\beta}^{(0)}(\alpha\xi)\equiv 0$. Here the superscript (n) identifies the iteration, and $\mathscr{A}^{-1}$ is the inverse of the matrix $\mathscr{A}$. The iterative procedure implied by (16) will yield $\boldsymbol{\beta}$ for many but not all problems.

3. Comparison with other work and with experiments

There have been many investigations of flow fields and heat transfer in constant-area ducts, both with and without mass transfer at the walls. These results can be compared with the application developed in appendix A. We shall begin by discussing the flow field, first considering flows without mass transfer and then flows with mass transfer. We close with some remarks about heat transfer.

3.1. *Entrance flow in a tube without heat or mass transfer*

The entrance flow field in a duct of circular cross-section without mass transfer has been discussed extensively in the literature. In the limit $k\to 0$, (A 2) and (A 3) approach the velocity and pressure fields that were called 'Targ-type' by Sparrow *et al.* (1964); the 'Targ-type' solution employs $U=u_0$ and does not satisfy an integral form of the mechanical energy conservation equation. The $k=0$ solid curves of figure 1 should therefore agree exactly with the points labelled 'Targ-type'. The very slight differences that are shown are indications of the errors in the solid curves of figure 1, which arise from truncating the series in (A 2) at $j=25$. These errors are not present in the results of Sparrow *et al.*

(even though a corresponding series was also truncated at $j = 25$) because it is possible to sum certain terms exactly when $k = 0$; in the present work, the truncation procedure employed for $k \neq 0$ was also used for $k = 0$ to facilitate comparison.

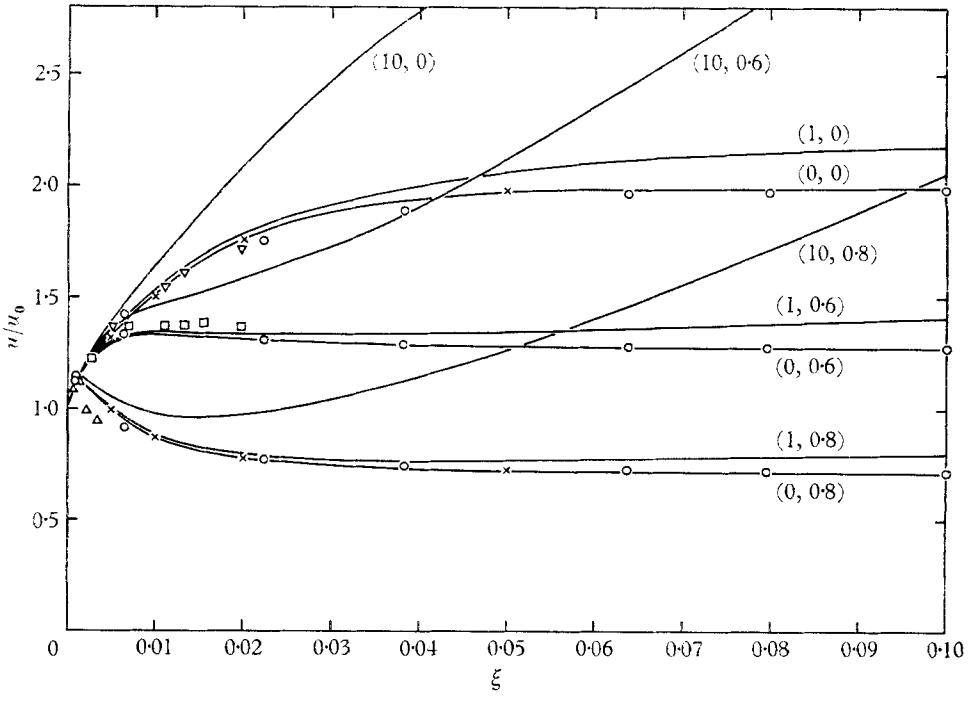

FIGURE 1. Axial development of velocity in a circular duct with uniform inlet conditions. Notation for curve labels is (k, η). Solid lines identify the present theory, ×, 'Targ-type' theory; ○, numerical calculation of Hornbeck. Experimental results of Aihara are identified by: ▽, (0, 0); □, (0, 0·6); △, (0, 0·8).

The points labelled 'numerical calculation' in figure 1 were obtained by Hornbeck (1963) from a finite-difference solution to the boundary-layer form of the governing partial differential equations for $k = 0$. These points, which probably represent the most accurate results currently available, differ at most by a few percent from the solid curves of figure 1 and agree almost exactly with the improved results of Sparrow *et al.*

The experimental points shown in figure 1 were obtained in recent hot-wire measurements, performed by Aihara for air flow through a porous-inlet tube, 30 in. long and 3 in. in diameter. They agree more closely with Hornbeck's points than with the solid lines, but they appear to exhibit radial profiles near the entrance that are slightly flatter in the centre of the duct than are the theoretical profiles. The accuracy of these experiments is comparable with or better than that of previously reported measurements; it is of the same order of magnitude as the difference between theory and experiment. Nevertheless, the systematic discrepancy between theory and experiment *may* point toward failure of the boundary-layer approximation.

$k\xi$ \ η	0	0·20	0·40	0·60	0·80	0·90	0·95
1×10^{-3}	1·04	1·04	1·04	1·04	1·04	1·04	1·004
2×10^{-3}	1·06	1·06	1·06	1·06	1·06	1·053	0·8917
5×10^{-3}	1·0942	1·0942	1·0942	1·0942	1·0938	1·0124	0·6887
1×10^{-2}	1·1360	1·1360	1·1360	1·1360	1·1224	0·9016	0·5408
2×10^{-2}	1·1979	1·1978	1·1978	1·1974	1·1079	0·7572	0·4214
5×10^{-2}	1·3300	1·3300	1·3288	1·2960	0·9913	0·5858	0·3115
1×10^{-1}	1·4926	1·4899	1·4639	1·3256	0·8824	0·4948	0·2597
2×10^{-1}	1·7095	1·6820	1·5723	1·3078	0·8023	0·4400	0·2299
5×10^{-1}	1·8718	1·8119	1·6243	1·2865	0·7622	0·4148	0·2164
1	1·8828	1·8206	1·6275	1·2850	0·7598	0·4133	0·2156
2	1·8829	1·8206	1·6275	1·2850	0·7597	0·4132	0·2156
5	1·8829	1·2806	1·6275	1·2850	0·7597	0·4132	0·2156

TABLE 1. Development of profiles of $(u/u_0)\, e^{-k\xi}$ for $k = 10$

3.2. *Entrance flow with mass transfer in a tube*

The curves for $k \neq 0$ shown in figure 1 represent portions of the results of calculations that were performed on the basis of the present theory. Given in table 1 is another sample of the theoretical velocity fields obtained from (A 2). The theory

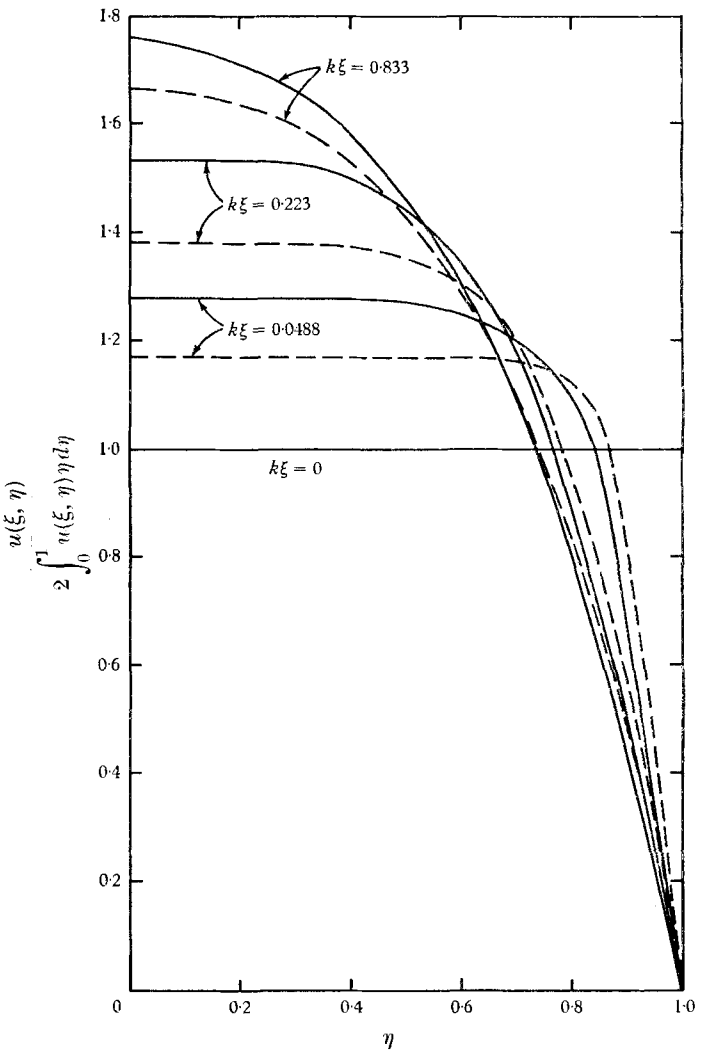

FIGURE 2. Comparison of development-zone velocity profiles with numerical results of Hornbeck *et al.*, for $k = 31{\cdot}416$. Dotted lines identify the present theory, solid lines Hornbeck *et al.*

predicts that the radial profiles of velocity tend to remain flatter when k is large than when k is small. Corresponding calculations have been reported by Hornbeck, Rouleau & Osterle (1963), who obtained finite-difference, numerical solutions to the boundary-layer form of the conservation equations for circular ducts with mass injection at the wall. Figure 2 shows a comparison of velocity

profiles given by the present theory with those of the numerical calculations, for flow development from a uniform inlet profile in a porous tube having $k = 10\pi$. The comparison shows that the present results exhibit somewhat broader profiles at this value of k. The pressure distributions are in better agreement, as is indicated below (for $k = 10\pi$):

$k\xi$	0·148	0·588	1·030
P, Hornbeck *et al.* (1963)	1·338	2·617	3·132
P, present theory	1·311	2·703	3·197

Here the reduced pressure is $P \equiv e^{-2k\xi}(p_0 - p)/(\frac{1}{2}\rho u_0^2)$. Listed in table 2 are additional pressure distributions obtained by first summing the series in (A 3) to $j = 25$, then using an asymptotic expansion for the roots of Bessel functions to evaluate the contribution to P from the terms $j > 25$.

k / $k\xi$	1	10	100	1000
1×10^{-3}	0·4035	0·1138	—	—
2×10^{-3}	0·5921	0·1706	—	—
5×10^{-3}	0·9878	0·2916	0·0959	—
1×10^{-2}	1·4660	0·4362	0·1479	—
2×10^{-2}	2·1947	0·6542	0·2381	—
5×10^{-2}	3·8424	1·1240	0·4522	0·2558
1×10^{-1}	6·1644	1·6900	0·7323	0·4564
2×10^{-1}	10·1439	2·4957	1·1620	0·7924
5×10^{-1}	18·2531	3·8701	1·9467	1·4512
1	24·4882	4·8475	2·4987	1·9418
2	27·6258	5·3356	2·7571	2·1825
5	28·1157	5·4118	2·7940	2·2197

TABLE 2. Pressure distributions for entrance flow with injection

Entrance flow with wall mass transfer also was analyzed by Weissberg (1959), who used the average technique of Morduchow (1957) (akin to a Kármán–Pohlhausen technique) to reduce the equations describing flow development in a circular duct to an ordinary differential equation (in x) that was integrated analytically. Since the method of Weissberg is applicable only to a one-parameter family of entrance velocity profiles that does not include the uniform velocity profile, comparison with the results that we have been discussing is not possible. Although we have chosen uniform initial profiles for all flow variables, our theory is easily generalized (by redefining the coefficients c_j and by introducing suitable changes in the method for calculating the β_i fields) to include arbitrary initial profiles that obey suitable symmetry conditions. In particular, (8) to (10) are easily modified to account for a parabolic initial velocity profile, which was the profile selected from the one-parameter family by Weissberg for presenting results. Corresponding numerical calculations by Hornbeck *et al.* (1963) are in good agreement with the results of Weissberg in this case. When the present theory is modified appropriately, it is found that with parabolic initial profiles $u(\xi, \eta)/u(\xi, 0) = 1 - \eta^2$ for all k and ξ; the shape of the velocity profile remains

invariant! This result does not differ greatly from many of the results of Weissberg, which show little change of the velocity profile in the entrance region except at high suction rates ($k < -10$), but the result does accentuate a shortcoming of the present linearization for $k \neq 0$: the velocity profile throughout the entire length of the duct, as predicted by generalizations of the present theory, depends on the entrance velocity profile when the wall injection rate is a constant ($\oint n.v ds = \text{const} \neq 0$). Other aspects of this difficulty will be emphasized in the following discussed of asymptotic ($\xi \to \infty$) flow properties.

3.3. *Fully developed flow with mass transfer in a tube*

Fully developed flow in a duct of circular cross-section, with constant wall mass transfer ($k = \text{const}$), was analyzed by Yuan & Finkelstein (1956), who discovered a similarity solution to the full Navier–Stokes equations for this problem. It is

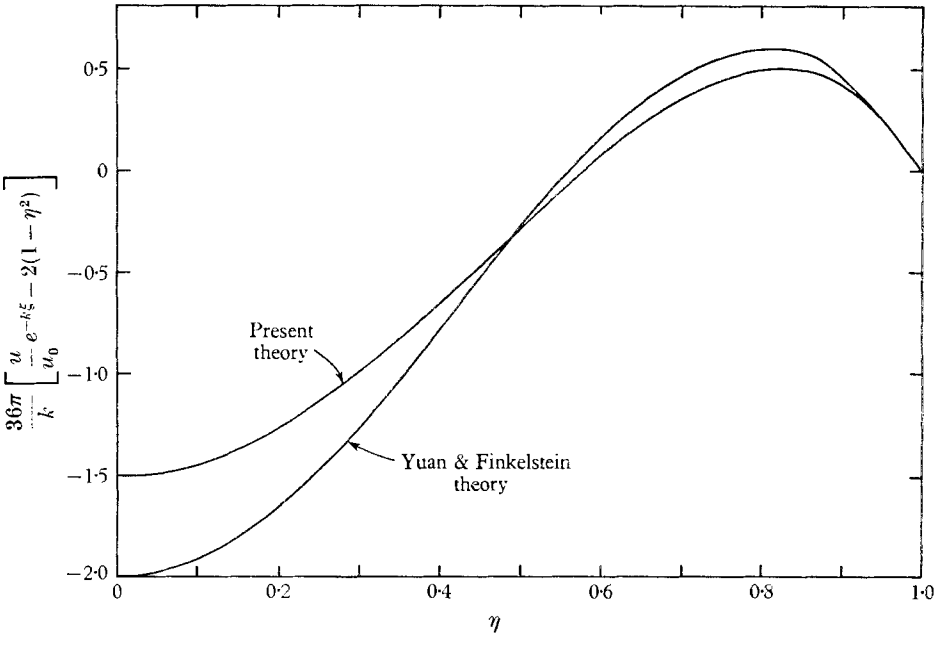

FIGURE 3. Comparison of coefficient of k in power-series expansion of velocity profile for fully developed flow in a circular duct.

generally agreed that at large distances downstream from the entrance plane ($k\xi \geqslant 1$), Yuan's results correctly describe the flow field, provided that k is sufficiently small ($k \ll 1$). Therefore it is of interest to compare our asymptotic ($k\xi \to \infty$) results for small values of k with the small-k results of Yuan. For the reduced pressure P, (A 3) yields

$$P = (8\pi/k) + 3 + (5k/16\pi) \times 0{\cdot}11126 + O(k^2),$$

while Yuan gives

$$P = (8\pi/k) + 3 + (5k/16\pi) \times 0{\cdot}26074 + O(k^2);$$

the first two terms in these expansions agree exactly, and the third terms agree in sign but differ in magnitude by a factor somewhat greater than 2. A comparison

of the fully developed, small-k velocity profile predicted by (A 2) with the corresponding result of Yuan is shown in figure 3, where the coefficients of the terms that are linear in k are plotted; the agreement is seen to be good. We might infer that for initially uniform velocity profiles the present analysis is likely to yield reasonably accurate flow fields at sufficiently small values of k. Extensions of the present analysis to non-uniform initial velocity profiles will not always yield accurate results for small k (e.g. for an initially parabolic profile, the theoretical curve in figure 3 would be identically zero).

Fully developed pipe flow at large values of $|k|$ presents a more complicated analytical problem. For the corresponding two-dimensional channel problem, Proudman (1960) and Terril (1964, 1965*a*) have shown that boundary layers develop on the walls for negative k and in the centre of the channel for positive k, thereby invalidating the analogue of Yuan's solution. These same phenomena occur in a duct of circular cross-section. For large negative values of k, these phenomena strongly modify the flow field, thereby negating the results of many earlier approximate analyses. Consequently, accurate flow fields are not known for large negative values of k, and we shall not consider this case. For large positive values of k, it turns out that the limiting ($k \to \infty$) solution of Yuan remains valid, but the correction terms (involving powers of $1/k$) for the velocity profile are likely to be in error near the centre of the duct (cf. Terril 1965*a*). In the limit $k \to \infty$, the fully developed, reduced pressure P given by the present theory (A 3) becomes

$$P = 2 + 4/(\pi k)^{\frac{1}{2}} + \ldots,$$

while Yuan obtains

$$P = 2{\cdot}4674 + (8\pi/k)(1{\cdot}3253) + \ldots;$$

these results differ numerically in the first term and functionally in the second. Yuan's result is probably the better of the two (although it too may be functionally incorrect), and therefore we may conclude that the present theory is poor for large values of k.

This conclusion is further supported by the velocity profiles shown in figure 4. The value of k employed in the experiment is so large that the corresponding fully developed velocity profile of an accurate theory is expected to differ by less than a percent or two from the profile of Yuan with $k = \infty$. Agreement between Yuan's theory and experiment is seen to be excellent, except in a small range of radius around $\eta = 0{\cdot}9$. The discrepancy in this range is not produced by inaccuracy in the theoretical fully developed velocity profile, because corrections to the theory can occur only near $\eta = 0$. Instead, the discrepancy is due to the fact that the experimental profiles are not quite fully developed; this interpretation is supported by the observation that increasing $u_0 A$ improves agreement. To explain why the experimental profile develops in the observed manner is likely to be difficult. The boundary-layer calculations of Hornbeck *et al.* (1963) produce profiles whose curvatures are always negative in the development region, but the experiment shows an inflexion point in the developing profile. An extension analogous to that of Atkinson and Goldstein (Goldstein 1938, p. 304), of the Boussinesq (1891) method of expanding about the fully developed flow seems best suited for attempting to explain the observations.

The present theory predicts that the experimental velocity profile should be essentially fully developed and should be much flatter than observed. The curve for $k = 100$ shown in figure 4 indicates that contrary to the results of the accurate theory, the fully developed profile of the present theory varies appreciably with k in this high-k régime. It can in fact be seen from (A 2) that the present

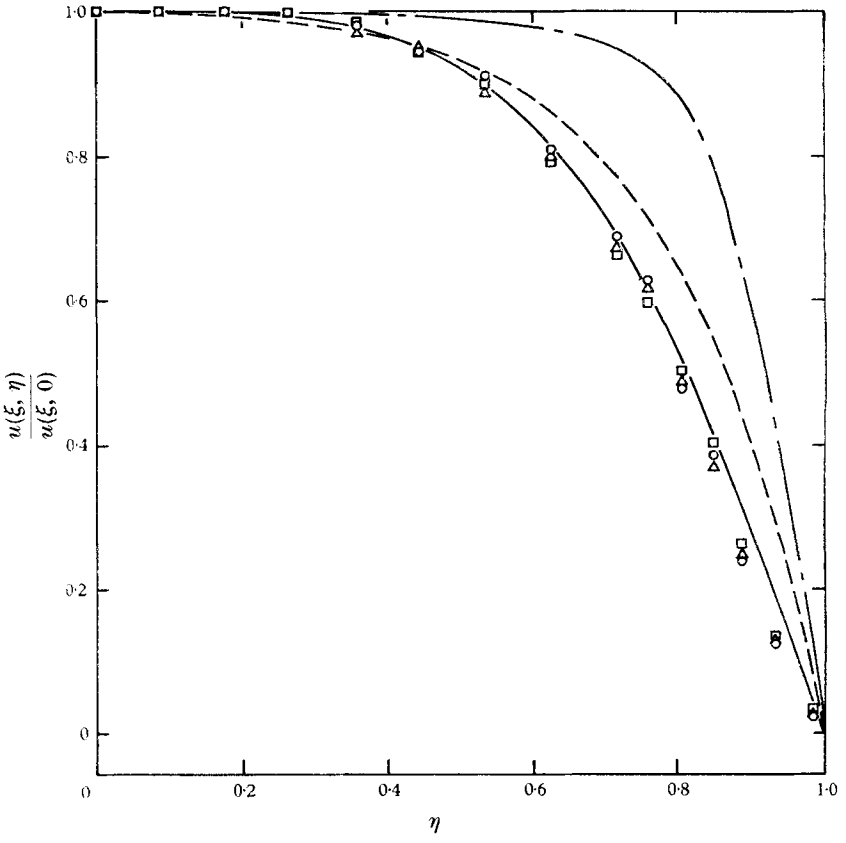

FIGURE 4. Velocity profiles for fully developed pipe flow at large values of k. Dotted line identifies the present theory for $k = 100$, broken line the present theory for $k = 425$, solid line Yuan &Finkelstein (1956) theory for $k = \infty$. Points correspond to Aihara experiments for $k = 425$, eight tube diameters downstream from entrance plane where ○, $u_0 A = 0$ cfm, △, $u_0 A = 1$ cfm, □, $u_0 A = 2$ cfm.

theory predicts that $u(\xi, \eta)/u(\xi, 0) \to 1$ as $k \to \infty$ for all values of ξ and η; i.e. the profile becomes perfectly flat and the development zone vanishes. Generalizations of the present theory to non-uniform initial profiles show that as $k \to \infty$ the development region always vanishes and the fully developed profile is always the same as the entrance profile (and therefore is not always flatter than the correct fully developed profile). These unreasonable results demonstrate clearly that the linearization is erroneous for large values of $|k|$, a conclusion which might have been premised from the observation that transverse inertial forces are large in the vicinity of the wall.

3.4. *Heat transfer in a tube with a fully developed velocity field*

Among the many possible heat transfer studies with which results of the present theory can be compared, we choose heat transfer in a fully developed velocity field for the small-k régime, in which the present velocity field is most accurate. Accurate results for this problem, in the case of a two-dimensional channel subjected to a step in wall temperature at a specified axial position, recently have been reported by Terril (1965*b*). We first consider the asymptotic ($\xi \to \infty$) heat transfer rate in a duct of circular cross-section whose walls are maintained at a constant temperature that differs from the inlet temperature of the fluid; the asymptotic heat transfer coefficient for this problem is the same as the asymptotic heat transfer coefficient that is achieved when a step in wall temperature is applied at any specified axial position. For the asymptotic Nusselt number based on tube diameter our theory gives

$$Nu = \frac{\gamma_1^4}{8\pi^2}\left[1 - \tfrac{1}{2}\gamma_1^2 k \sum_{j=1}^{\infty} (\alpha_j^2 + k)^{-1}(\alpha_j^2 - \gamma_1^2)^{-1}\right]^{-1},$$

where α_j and $\gamma_1 = 2{\cdot}4048\sqrt{\pi}$ are the eigenvalues defined in appendix A. For $k = 0$, this formula yields $Nu = 4{\cdot}18$, a value which does not differ too greatly from the result of Nusselt (1910), $Nu = 3{\cdot}66$, obtained from a numerical integration of the partial differential equation that describes the temperature field.

The value of Nu predicted by the present theory is monotonic in k and approaches $\gamma_1^2/\pi = 5{\cdot}783$ as $k \to \infty$. Therefore the value of Nu is found to depend only weakly on k for $k \geqslant 0$, but the value increases as k increases. This dependence is a direct consequence of the change in the u field as k changes, and it enters only through the definition of the average temperature difference,

$$\bar{\beta} - \beta_w = \iint (\beta - \beta_w) u \, dA \Big/ \iint u \, dA,$$

which decreases as k increases. In the correct physical description of the system, this dependence is counteracted by a decrease in the rate of heat transfer due to a modification of the temperature profile caused by inward radial convection. This convective effect, which is not included in the present theory, is generally larger than the effect due to the change in $\bar{\beta}$, and therefore the sign of $\partial Nu/\partial k$ given by the present theory is incorrect. Furthermore, the present theory predicts that Nu is independent of the Prandtl number α, a result which almost certainly is incorrect for all $k \neq 0$; see Terril (1965*b*). We may therefore conclude that the description of the temperature field provided by the present theory, for heat transfer to an isothermal wall, is inaccurate when mass transfer occurs through the walls. Hence, there is no justification for proceeding to make more detailed comparisons of the present results with other theories for problems of this type. This unfavourable result does not necessarily imply that the theory will be inaccurate for the applications considered in appendices *B*, *C* and *D*.

In summary, it may be stated that the theory presented herein produces reasonably accurate velocity and pressure fields for duct flows with wall injection, provided that the Reynolds number based on injection velocity is

sufficiently small. At large injection Reynolds numbers, the present theory is highly inaccurate, especially for the velocity field. Furthermore, the temperature field in a duct with isothermal walls is described poorly by the present theory, unless the Reynolds number based on injection velocity is zero.

The author wishes to thank the Air Force Office of Scientific Research for providing support for this work through Grant no. AF-AFOSR-927-66 and Y. Aihara for making his experimental results available for comparison with this theory prior to their publication. Thanks are also extended to many of my UCSD colleagues, particularly D. R. Kassoy, P. A. Libby and J. W. Miles, for helpful discussions concerning this problem.

Appendix A. Entrance flow with heat transfer to an isothermal wall

Consider the entrance flow of a one-component gas which has a temperature T_0 at $x = 0$ and a constant temperatre T_w at the walls of the duct. A specified wall area variation and a specified rate of injection at the wall are both permitted. In this case there is only one coupling function β, which may be taken to be the thermal enthalpy of the gas. The solution for the temperature field is given most conveniently by (14*a*), in which $\beta_{wz} = (\beta_w - \beta_0)\delta(z)$, where β_w is a known constant. Thus,

$$\beta = \beta_0 + (\beta_w - \beta_0) G_A(\alpha\xi, r). \tag{A 1}$$

The solution for the velocity field is given by (8), in which $F(\xi)$ is a prescribed function. For a circular cross-section,

$$G_A = 1 - \sum_{j=1}^{\infty} a_j J_0(\gamma_j r) \exp(-\gamma_j^2 \alpha\xi),$$

where J_0 is the zero-order Bessel function of the first kind, γ_j are the roots of

$$J_0(\gamma/\sqrt{\pi}) = 0,$$

and the coefficients a_j are given by

$$a_j = \int_0^{1/\sqrt{\pi}} J_0(\gamma_j r)\, r\, dr \Big/ \int_0^{1/\sqrt{\pi}} [J_0(\gamma_j r)]^2 r\, dr = (2\sqrt{\pi}/\gamma_j)[J_1(\gamma_j/\sqrt{\pi})]^{-1}.$$

The example cited here serves to illustrate a number of drawbacks of the present theory. Even when the cross-sectional area of the duct is constant and the questionable approximation (3) does not appear, mass addition merely alters the axial location at which a particular temperature profile is attained, without influencing the shape of the temperature profile. In other words, both γ_j and the coefficient of $\exp(-\gamma_j^2\alpha\xi)$ in G_A are independent of $F(\xi)$. It is clear on physical grounds that local mass addition must modify the shape of the radial temperature profile in the vicinity of the wall, because of the consequent radial convection. This effect does not appear in the present formulation. The theory is closer than desirable to a quasi-one-dimensional theory.

It is of interest to calculate explicitly the velocity profiles and pressure gradient in a constant-area duct of circular cross-section, with a constant value of the non-dimensional rate k at which mass is injected through the wall. The quantity k is defined as the ratio of the mass injected per unit duct length per second to the coefficient of viscosity. Positive values of k correspond to blowing, negative values to suction. Employing (11), one finds from (6), (7) and (8) that

$$U = u_0 + kx, \quad e^{k\xi} = 1 + kx/u_0, \quad F(\xi) = k\,e^{k\xi},$$

and

$$u = 2u_0(1-\eta^2)\,e^{k\xi} + 4\pi u_0 \sum_{j=1}^{\infty} \frac{1}{\alpha_j^2}\left[\frac{J_0(\alpha_j\eta/\sqrt{\pi})}{J_0(\alpha_j/\sqrt{\pi})} - 1\right]\exp(-\alpha_j^2\xi)\left\{1 + \left(1+\frac{\alpha_j^2}{k}\right)^{-1}[\exp\{(\alpha_j^2+k)\xi\} - 1]\right\}, \tag{A 2}$$

where α_j are the positive roots of $J_2(\alpha_j/\sqrt{\pi}) = 0$, and $\eta \equiv r/r_0$, $r_0 = 1/\sqrt{\pi}$ being the duct radius. Equations (2) and (A 2) show that

$$\frac{p_0 - p}{\frac{1}{2}\rho u_0^2} = \left(\frac{8\pi}{k} + 2\right)(e^{2k\xi} - 1) + \sum_{j=1}^{\infty}\left(\frac{8\pi}{k+\alpha_j^2}\right)\left\{\left(\frac{\alpha_j^2}{k-\alpha_j^2}\right)[\exp\{(k-\alpha_j^2)\xi\} - 1] + \tfrac{1}{2}(e^{2k\xi} - 1) + [\alpha_j^2/(k+\alpha_j^2)](e^{k\xi} - \exp(-\alpha_j^2\xi))^2\right\}. \tag{A 3}$$

Equation (A 3) agrees with the corresponding result given by Sparrow, *et al.* (1964) in the limit $k \to 0$ and approaches a 'fully developed' limit of

$$\left[\frac{8\pi}{k} + 2 + 4\pi \sum_{j=1}^{\infty} \frac{k + 3\alpha_j^2}{(k+\alpha_j^2)^2}\right] e^{2k\xi}$$

as $k\xi \to \infty$ (implying a quadratic decrease of pressure with distance).

Appendix B. Constant rate of injection of a foreign gas

Consider flow of a two-component non-reacting gas through a duct. Pure species 1 enters at $x = 0$, and pure species 2 is injected at a constant rate (mass per unit length per second) through the wall; it should be clear from the results how to remove the restrictions to pure species. It is appropriate here to let β_i be the mass fraction of species i. Since $\beta_1 + \beta_2 = 1$, we need to solve for only one of the β fields. Choosing β_1, we have the boundary conditions $\beta_1 = 1$ at $x = 0$ and $\mathbf{n}.\mathbf{v}\beta_1 = \alpha\mathbf{n}.\boldsymbol{\nabla}\beta_1$ at the wall. The last of these conditions is of the form of (12), with $C_1 = 0$, $B_{11} = 1$, $A_{11} = -(\mathbf{n}.\mathbf{v})_w/\alpha$. The solution for β_1 may be calculated from the iterative procedure defined in (16). However, for the present problem, and indeed whenever all elements of A_{ki}, B_{ki} and C_k are constant, iteration can be avoided by adopting a slightly different procedure.

The present problem can be written in the form

$$\partial\beta_1/\partial(\alpha\xi) = \nabla^2\beta_1;$$
$$\beta_1 = 1 \quad \text{for} \quad \xi \leqslant 0,$$
$$A_{11}\beta_{1w} + (\mathbf{n}.\boldsymbol{\nabla}\beta_1)_w = 0 \quad \text{for} \quad \xi > 0.$$

Let h_j be eigenfunctions and δ_j be eigenvalues of the two-dimensional problem

$$\delta_j^2 h_j + \nabla^2 h_j = 0,$$

$$A_{11} h_{jw} + (\mathbf{n}.\nabla h_j)_w = 0.$$

Then
$$\beta_1 = \sum_j h_j \exp(-\delta_j^2 \alpha \xi) \iint h_j dA \Big/ \iint h_j^2 dA.$$

For a duct with a circular cross-section of initial radius r_0, we find that

$$h_j = J_0(\delta_j \eta/\sqrt{\pi}),$$

where $\eta \equiv r/r_0$ and δ_j are the roots of

$$J_0(\delta_j/\sqrt{\pi}) = (\delta_j/A_{11}) J_1(\delta_j/\sqrt{\pi}).$$

In this case, the solution for β_1 becomes

$$\beta_1 = \sum_{j=1}^{\infty} J_0(\delta_j \eta/\sqrt{\pi}) \exp(-\delta_j^2 \alpha \xi) \int_0^1 \eta J_0(\delta_j \eta/\sqrt{\pi}) d\eta \Big/ \int_0^1 \eta [J_0(\delta_j \eta/\sqrt{\pi})]^2 d\eta. \quad \text{(B 1)}$$

The eigenvalues δ_j can be computed numerically; their values will depend on the value of A_{11}. Since $A_{11} > 0$ by definition in this problem, all eigenvalues are positive.

It may be remarked that (A 2), (A 3) and (B 1) provide solutions for the velocity, pressure and concentration field in a constant-area duct of circular cross-section, with a constant rate of injection of a foreign gas; the transverse velocity can be obtained from the axial velocity by integrating (1*a*). The same formulas provide solutions for the velocity, pressure and temperature fields in a constant-area duct of circular cross-section, with a constant rate of injection of a gas which has a constant temperature differing from that of the inlet gas. This conclusion follows from the observation that the quantity $(h - h_2)/(h_1 - h_2)$ (where h is thermal enthalpy per unit mass, the subscript 1 identifies the inlet gas, and the subscript 2 identifies the gas injected through the wall) obeys precisely the same differential equation and boundary conditions that β_1 obeys. Subject to the basic hypothesis that the diffusivity α is a known constant, the solution for the enthalpy field is independent of the chemical composition of the non-reacting inlet and injected gases. Thus, the entire flow field has been determined for the problem of a constant-area duct with a constant rate of injection of a foreign gas at a temperature differing from that of the inlet gas.

Appendix C. Vaporization or sublimation of the wall material

Consider a two-component, non-reacting gas, with pure species 1 entering at $x = 0$ and species 2 maintaining phase equilibrium at a solid or liquid wall. The wall injection rate depends on solutions for the coupling functions.

It is convenient to let β_1 represent the mass fraction of species 1 and β_2 denote the ratio of the local thermal enthalpy (per unit mass) to the thermal enthalpy (per unit mass) at $x = 0$. Boundary conditions for the two coupling-function fields then become $\beta_1 = \beta_2 = 1$ at $x = 0$ and

$$(\alpha \mathbf{n}.\nabla \beta_1)_w = (\mathbf{n}.\mathbf{v}\beta_1)_w, \quad (\alpha \mathbf{n}.\nabla \beta_2)_w = (\mathbf{n}.\mathbf{v}l)_w \quad \text{(C 1)}$$

at the wall. In the last expression, l is the ratio of the heat required per unit mass for gasification of species 2 to the thermal enthalpy per unit mass at $x = 0$ and is assumed to be a known constant. These boundary conditions are sufficient for determining both β fields in terms of the unknown injection rate $(\mathbf{n}.\mathbf{v})_w$, thus yielding formulas for β_{1w} and β_{2w} in particular.

The phase equilibrium condition provides an additional independent relationship among β_{1w}, β_{2w} and $(\mathbf{n}.\mathbf{v})_w$, thereby determining the injection rate. The equation for phase equilibrium is obtained by setting the partial pressure of species 2 at the wall equal to its equilibrium vapour pressure p_e. The equilibrium vapour pressure p_e at the wall is a known function of the wall temperature, which in turn is a known function of β_{2w}; i.e. $p_e = p_e(\beta_{2w})$. Relating mass fractions to mole fractions, we then find

$$(1-\beta_{1w})p/[1+(w-1)\beta_{1w}] = p_e(\beta_{2w}) \tag{C 2}$$

to be the formal expression for wall equilibrium, where w is the ratio of the molecular weight of species 2 to that of species 1. The pressure p which appears in (C 2) is to be obtained from the integral of (2); p therefore depends on $(\mathbf{n}.\mathbf{v})_w$.

The boundary conditions for β_2 are such that an expression for β_2 (and hence for β_{2w}) can be written from (14*b*). The expression involves $(\mathbf{n}.\mathbf{v})_w$ and integrals of it. Also, (8) may be utilized to integrate (2), thereby providing a closed-form, infinite-series expression for p in terms of $(\mathbf{n}.\mathbf{v})_w$ and various of its integrals. Equation (C 2) therefore can be solved for β_{1w} in terms of $(\mathbf{n}.\mathbf{v})_w$ and its integrals. The resulting formula and the boundary condition for β_1 at $x = 0$ can be used in (14*a*) to provide a complicated, closed-form expression for the β_1 field in terms of $(\mathbf{n}.\mathbf{v})_w$ and its integrals. The first boundary condition in (C 1) then will yield a single integral equation for $(\mathbf{n}.\mathbf{v})_w$. The final integral equation will not possess a simple analytical solution.

There are numerous special conditions under which this complicated procedure can be simplified. These include cases in which $(p_0-p)/p_0 \ll 1$ for all x and cases in which $(U-u_0)/U \ll 1$ for all x. Instead of attempting to discuss all possible limiting cases, we shall discuss only the case in which $p_e(\beta_{2w})$ depends so strongly on surface temperature that the solution to (C 2) yields a very small change in β_{2w} over the entire range of variation of p and β_{1w} within the duct. Heats of gasification are often high enough for this to be true. Equation (C 2) then reduces approximately to

$$\beta_{2w} = \text{constant};$$

the wall temperature is approximately equal to a constant equilibrium vaporization or sublimation temperature. We shall consider the consequences of treating β_{2w} as a known, specifiable constant.

With β_{2w} = constant, the temperature fields is given explicitly by (A 1). The second boundary condition in (C 1) then yields the gasification rate $(\mathbf{n}.\mathbf{v})_w$ directly; neither velocity, pressure nor concentration fields need be considered in calculating the gasification rate, but in general (e.g. if the cross-sectional area is specified function of x) an integral equation must still be solved to express the gasification rate as a function of x instead of ξ. Having obtained the gasification rate, we can calculate the velocity and pressure fields from (8) and from the

integral of (2). The first boundary condition in (C 1) and the condition on β_1 at $x = 0$ serve to determine the composition field, which in this case can be calculated most easily by the iterative procedure given in (16).

As an example, for a circular cross-section we have

$$\beta_2 = \beta_{2w} + (1-\beta_{2w}) \sum_{j=1}^{\infty} (2\sqrt{\pi}/\gamma_j)[J_0(\gamma_j r)/J_1(\gamma_j/\sqrt{\pi})] \exp(-\gamma_j^2 \alpha \xi),$$

where $\gamma_j (> 0)$ are given by $J_0(\gamma_j/\sqrt{\pi}) = 0$, whence the second boundary condition in (C 1) yields

$$k \equiv 2\pi r_0 b(-\mathbf{n}.\mathbf{v})_w = b[4\pi\alpha(1-\beta_{2w})/l] \sum_{j=1}^{\infty} \exp(-\gamma_j^2 \alpha \xi) \tag{C 3}$$

for the mass gasified per unit length of duct per second. If the approximation $U = u_0$ is introduced into the definition (6) of ξ, then (C 3) yields k explicitly as a function of x. This approximation will not be very accurate in the downstream portion of the duct if the total mass entering through the wall is comparable with or greater than the mass entering at $x = 0$. In such cases, the approximation still can be employed to initiate an obvious iterative computation of $k(x)$, utilizing alternately first (C 3) and then (11)

$$\text{viz. } U = u_0 + \int_0^x k\,dx.$$

If the cross-sectional area of the duct is constant, then (C 3) gives k explicitly as a function of ξ, and transformation back to the original co-ordinate x can be accomplished by means of the formula

$$x = u_0 \int_0^{\xi} \exp\left\{\int_0^{\xi'} k(\xi'')\,d\xi''\right\} d\xi',$$

which can be derived from (6) and (11).

Appendix D. Gas-phase combustion of the wall material

Suppose that the wall consists of a fuel F, that an oxidizer O enters at $x = 0$ and that the exothermic reaction $\nu_F F + \nu_O O \rightarrow \nu_P P$ can occur in the gas phase. We set $\beta_i (i = 1, 2, 3)$ equal to the thermal enthalpy-oxidizer concentration coupling function for $i = 1$, the fuel concentration-oxidizer concentration coupling function for $i = 2$, and the product concentration-oxidizer concentration coupling function for $i = 3$; to obtain dimensionless coupling functions, we multiply the β_i of Williams (1965) by $\nu_O W_O$, where W_O is the molecular weight of the oxidizer. Boundary conditions at $x = 0$ then become $\beta_{20} = \beta_{30} = 1$, $\beta_{10} - 1 =$ thermal enthalpy per unit mass of the entering (oxidizer) gas divided by the standard heat liberated in the reaction per unit mass of oxidizer consumed. We assume that the isothermal wall approximation of appendix C is applicable and that gas-phase reaction rates are sufficiently fast for the oxidizer concentration at the wall to be negligibly small. The wall boundary conditions then become

$$\left.\begin{aligned} &\beta_{1w} = \text{constant}, \quad (\alpha\mathbf{n}.\nabla\beta_1)_w = (\mathbf{n}.\mathbf{v}L)_w, \\ &(\alpha\mathbf{n}.\nabla\beta_2)_w = [\mathbf{n}.\mathbf{v}(\nu+\beta_2)]_w, \quad (\alpha\mathbf{n}.\nabla\beta_3)_w = (\mathbf{n}.\mathbf{v}\beta_3)_w, \end{aligned}\right\} \tag{D 1}$$

where β_{1w} is the known ratio of the thermal enthalpy at the wall to the standard heat of reaction per unit mass of oxidizer, L is the ratio of the heat of gasification per unit mass to the standard heat of reaction per unit mass of oxidizer, and $\nu \equiv \nu_O W_O / \nu_F W_F$ is the stoichiometric mixture ratio.

From the first two expressions in (D 1) and from the fact that β_{10} is known, it will be noted that the problems of computing the β_1 field and the wall gasification rate are precisely the same as the corresponding simplified, isothermal-wall problems of appendix C. Therefore, the gasification rate problem requires no further discussion [e.g. (C 3) can be obtained, with $(1-\beta_{2w})/l$ replaced by $(\beta_{20}-\beta_{2w})/L$]. Velocity and pressure fields can be calculated from (8) and (2); the next-to-last condition in (D 1) (along with $\beta_{20} = 1$) may be used to obtain the β_2 field through (16); the last condition in (D 1) (along with $\beta_{30} = 1$) may be used to obtain the β_3 field through (16). Temperature and concentration fields follow from these results only in a flame-surface approximation. It would be of interest to calculate flame shapes, which are given by the equation $\beta_2 = 0$, but since the β_2 field is calculated iteratively, only a first iterative approximation to the flame shape can be obtained in closed form.

Although an appreciable amount of numerical work is necessary in obtaining complete solutions, these solutions contain a great deal of information. For example, one could trace the flame from the lip of the duct to the downstream point at which it reaches the centre line, follow the axial decay of oxidizer concentration along the centre line, observe how the centre-line temperature rises at first and then falls after passing the flame, obtain the asymptotic approach to an isothermal, fuel-rich flow with vanishing gasification rate, etc.

REFERENCES

Boussinesq, J. 1891 *Comptes Rendus*, **113**, 49.

Carrier, G. F. 1962 On the integration of equations associated with problems involving convection and diffusion. *Proceedings of the Tenth International Congress of Applied Mechanics*, Stressa, Italy, 1960. Amsterdam: Elsevier.

Cole, J. D. 1968 *Perturbation Methods in Applied Mathematics*. Waltham, Mass.: Blaisdell.

Goldstein, S. 1938 *Modern Developments in Fluid Mechanics*, vol. 1. Oxford: Clarendon Press.

Hornbeck, R. W. 1963 *Appl. Sci. Res.* 13 A, 224.

Hornbeck, R. W., Rouleau, W. T. & Osterle, F. 1963 *Phys. Fluids*, **6**, 1649.

Lewis, J. A. & Carrier, G. F. 1949 *Quart. Appl. Math.* **7**, 228.

Morduchow, M. 1957 *Quart. Appl. Math.* **14**, 361.

Nusselt, W. 1910 *Z.V.D.I.* **54**, 1154.

Oseen, C. W. 1910 *Arkiv. Math. Astron. Fysik.* **6**, 1.

Proudman, I. 1960 *J. Fluid Mech.* **9**, 593.

Sparrow, E. M., Lin, S. H. & Lundgren, T. S. 1964 *Phys. Fluids*, **7**, 338.

Terril, R. M. 1964 *Aeron. Quart.* **15**, 299.

Terril, R. M. 1965*a* *Aeron. Quart.* **16**, 323.

Terril, R. M. 1965*b* *Int. J. Heat Mass Trans.* **8**, 1491.

Weissberg, H. L. 1959 *Phys. Fluids*, **2**, 510.

Williams, F. A. 1965 *Combustion Theory*. Reading, Mass: Addison-Wesley.

Williams, J. C. III. 1963 *AIAA J.* **1**, 186.

Yuan, S. W. & Finkelstein, A. B. 1956 *Trans. ASME* **78** 719.